

## Supplemental Information

### Liquid structure of primary ammonium nitrate ionic liquids studied by high-energy X-ray diffraction experiments and MD simulations

Xuedan Song<sup>†</sup>, Hiroshi Hamano<sup>†</sup>, Babak Minofar<sup>†</sup>, Ryo Kanzaki<sup>‡</sup>, Kenta Fujii<sup>§</sup>, Yasuo Kameda<sup>⊥</sup>, Shinji Kohara<sup>#</sup>, Masayoshi Watanabe<sup>¶</sup>, Shin-ichi Ishiguro<sup>†</sup> and Yasuhiro Umebayashi<sup>\*,†</sup>

<sup>†</sup>Department of Chemistry, Faculty of Science, Kyushu University, Hakozaki, Higashi-ku, Fukuoka 812-8581, Japan.

<sup>‡</sup>Graduate School of Science and Engineering, Kagoshima University, Korimoto, Kagoshima 890-0065, Japan.

<sup>§</sup> Neutron Science Laboratory, Institute for Solid State Physics, The University of Tokyo, Kashiwanoha, Kashiwa-shi, Chiba 277-8581, Japan.

<sup>⊥</sup> Department of Material and Biological Chemistry, Faculty of Science, Yamagata University, Kojirakawa-machi 1-4-12, Yamagata 990-8560, Japan.

<sup>#</sup> Japan Synchrotron Radiation Research Institute (JASRI), Sayo-cho, Sayo-gun, Hyogo 679-5198, Japan.

<sup>¶</sup> Department of Chemistry and Biotechnology, Yokohama National University, 79-5 Tokiwadai Hodogaya-ku, Yokohama 240-8501, Japan.

\* Corresponding author. E-mail: [yumeb@chem.kyushu-univ.jp](mailto:yumeb@chem.kyushu-univ.jp)

**Table S1.** Lennard-Jones parameters and partial atomic point charges for  $[C_nAm^+]$  ( $n = 2, 3$ , and  $4$ ) and nitrate ions.

ammonium				nitrate			
atoms	$\sigma / \text{\AA}$	$\varepsilon / \text{kcal mol}^{-1}$	$q / e$	atoms	$\sigma / \text{\AA}$	$\varepsilon / \text{kcal mol}^{-1}$	$q / e$
CT	3.50	0.066	-0.18	NN	3.25	0.170	0.905
CS	3.50	0.066	-0.12	ON	2.96	0.210	-0.635
CE	3.50	0.066	-0.05				
C2	3.50	0.066	0.01				
C1	3.50	0.066	0.04				
N3	3.25	0.170	-0.36				
HC	2.50	0.030	0.06				
H1	2.50	0.030	0.13				
HN	2.50	0.030	0.31				

**Table S2.** The experimental density and simulated data of  $[C_nAm^+][NO_3^-]$  ( $n = 2, 3$ , and  $4$ ).

$n$	$\rho_{\text{obs.}} / \text{g cm}^{-3}$	$\rho_{\text{MD}} / \text{g cm}^{-3}$	$\Delta\rho / \%$
2	1.2109(1)	1.224(5)	1.1
3	1.1620(1)	1.158(5)	0.3
4	1.1089(1)	1.104(4)	0.4

**Figure S1.**

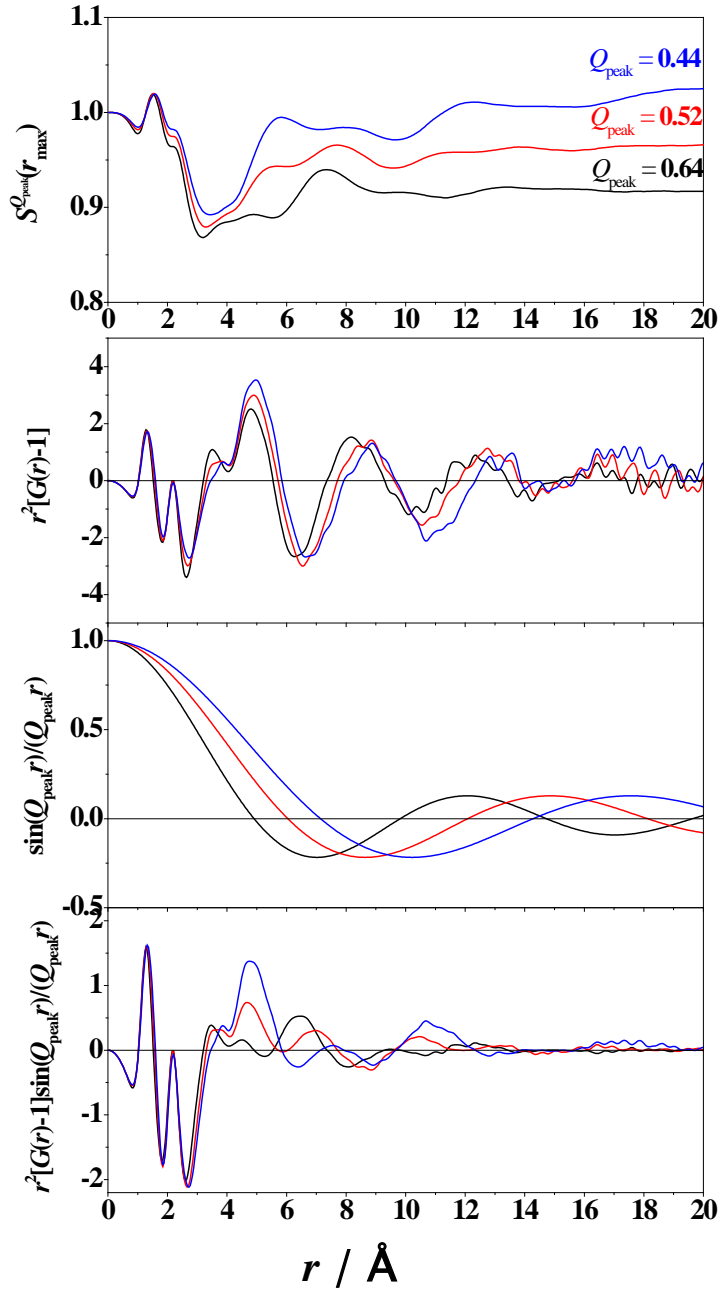


**Figure S1.**  $S^{Q_{\text{peak}}}(r_{\max})$  ,  $r^2[G(r)-1]$  ,  $\frac{\sin(Q_{\text{peak}}r)}{Q_{\text{peak}}r}$  and  $r^2[G(r)-1]\frac{\sin(Q_{\text{peak}}r)}{Q_{\text{peak}}r}$

with  $Q_{\text{peak}} = 0.64 \text{ \AA}^{-1}$  for  $[\text{C}_2\text{Am}^+][\text{NO}_3^-]$  (black),  $0.52 \text{ \AA}^{-1}$  for  $[\text{C}_3\text{Am}^+][\text{NO}_3^-]$  (red) and  $0.44 \text{ \AA}^{-1}$  for  $[\text{C}_4\text{Am}^+][\text{NO}_3^-]$  (blue) obtained by the HEXRD experiments.

**Figure S2.**

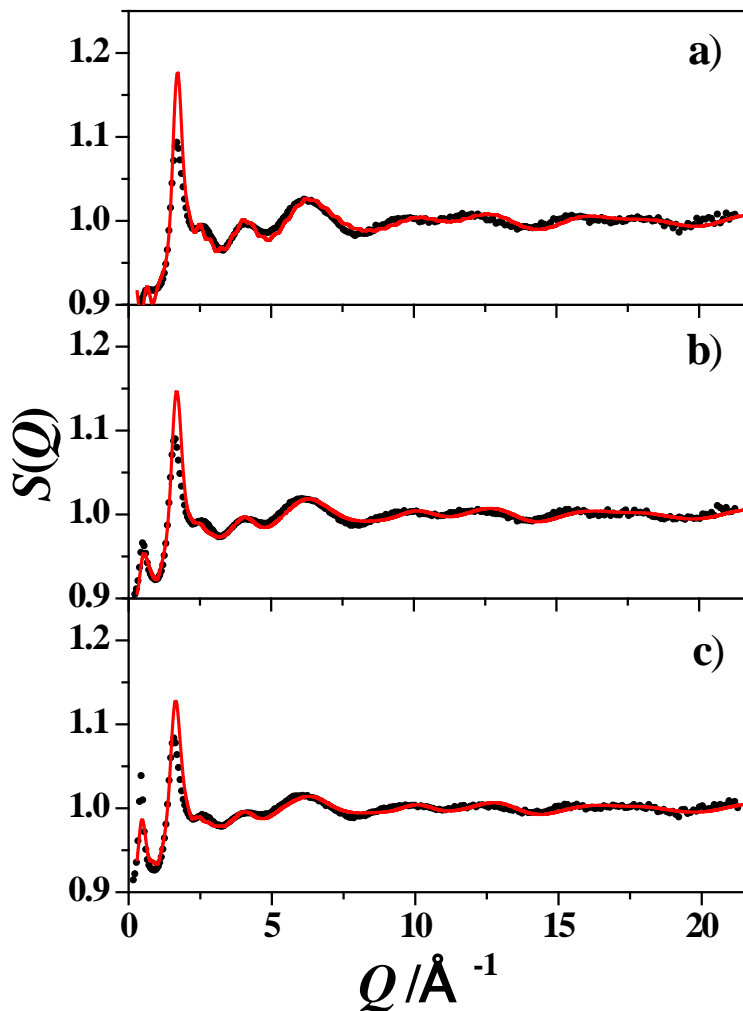


**Figure S2.** X-ray structure factors  $S(Q)$  obtained from the HEXRD experiments (black dots) and MD simulations (a red line) for protic ionic liquids: (a)  $[\text{C}_2\text{Am}^+]\text{[NO}_3^-]$ , (b)  $[\text{C}_3\text{Am}^+]\text{[NO}_3^-]$ , and (c)  $[\text{C}_4\text{Am}^+]\text{[NO}_3^-]$ .

**Figure S3.**

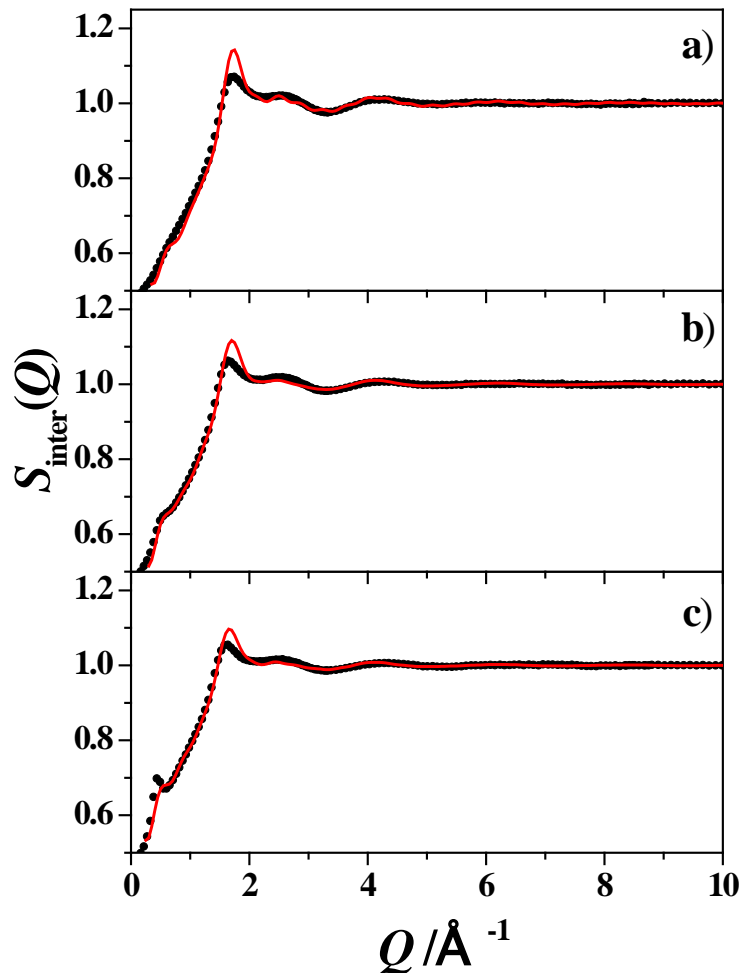


**Figure S3.** Inter-molecular structure factors  $S_{\text{inter}}(Q)$  extracted from the HEXRD experiments (black dots) and derived from MD simulations (a red line) for (a)  $[\text{C}_2\text{Am}^+]\text{[NO}_3^-]$ , (b)  $[\text{C}_3\text{Am}^+]\text{[NO}_3^-]$ , and (c)  $[\text{C}_4\text{Am}^+]\text{[NO}_3^-]$ .

**Figure S4.**

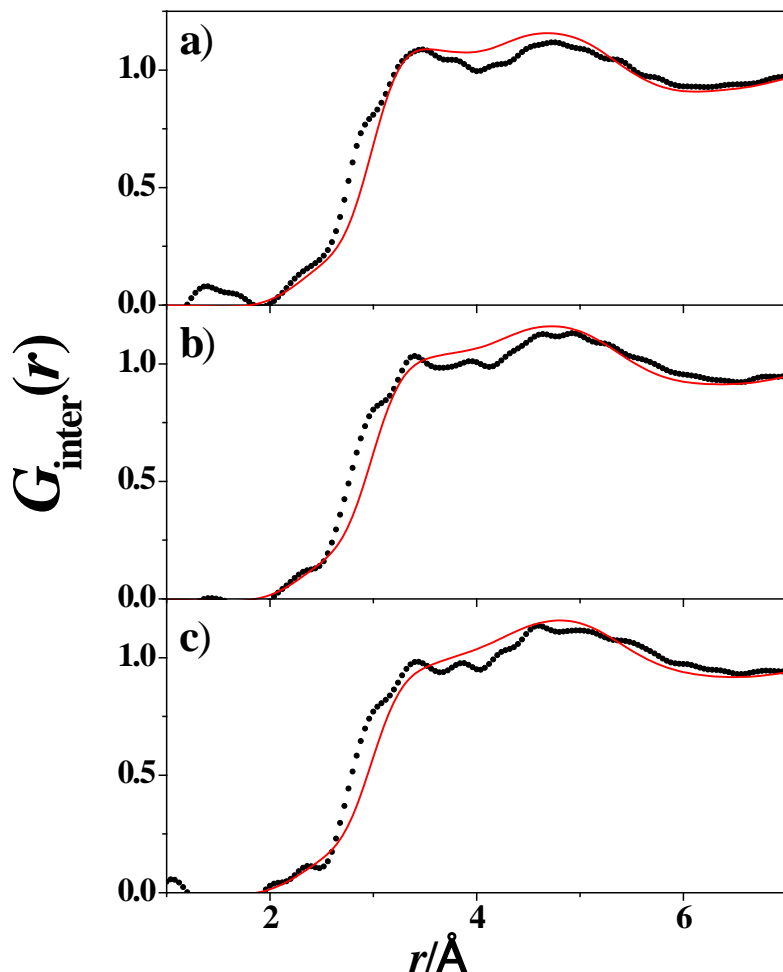


**Figure S4.** Inter-molecular X-ray radial distribution functions  $G_{\text{inter}}(r)$  extracted by the HEXRD experiments (black dots) and derived from MD simulations (a red line) for (a)  $[\text{C}_2\text{Am}^+][\text{NO}_3^-]$ , (b)  $[\text{C}_3\text{Am}^+][\text{NO}_3^-]$ , and (c)  $[\text{C}_4\text{Am}^+][\text{NO}_3^-]$ .

**Figure S5.**

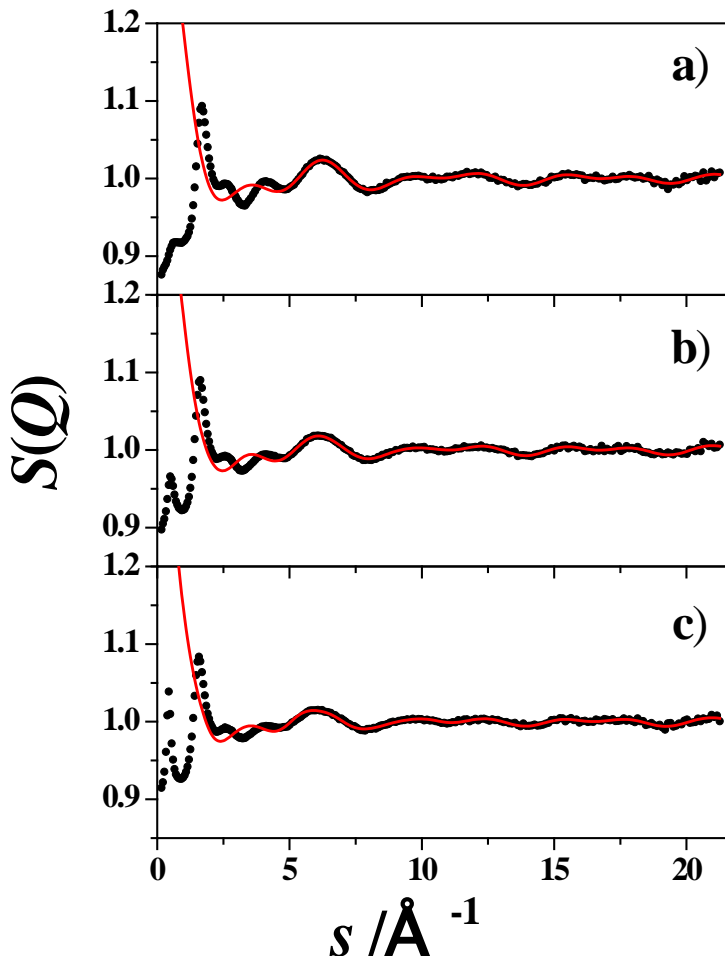


**Figure S5.** X-ray structure factors  $S(Q)$  obtained by the HEXRD experiments (black dots) and the intra-molecular structure factors estimated based on the molecular geometries found in crystal structure also shown as a red line. (a)  $[\text{C}_2\text{Am}^+][\text{NO}_3^-]$ , (b)  $[\text{C}_3\text{Am}^+][\text{NO}_3^-]$ , and (c)  $[\text{C}_4\text{Am}^+][\text{NO}_3^-]$ .

**Figure S6.**

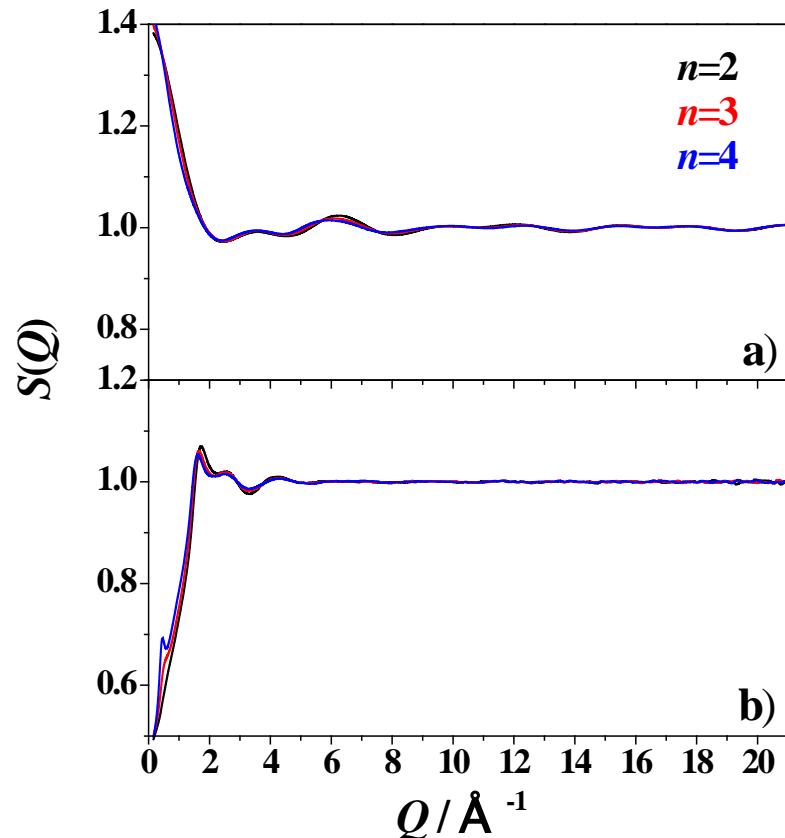


**Figure S6.** The intra- (a) and inter- (b) molecular structure factors obtained by the HEXRD experiments,  $[\text{C}_2\text{Am}^+]\text{[NO}_3^-]$  (black),  $[\text{C}_3\text{Am}^+]\text{[NO}_3^-]$  (red), and  $[\text{C}_4\text{Am}^+]\text{[NO}_3^-$  (blue).

**Figure S7.**

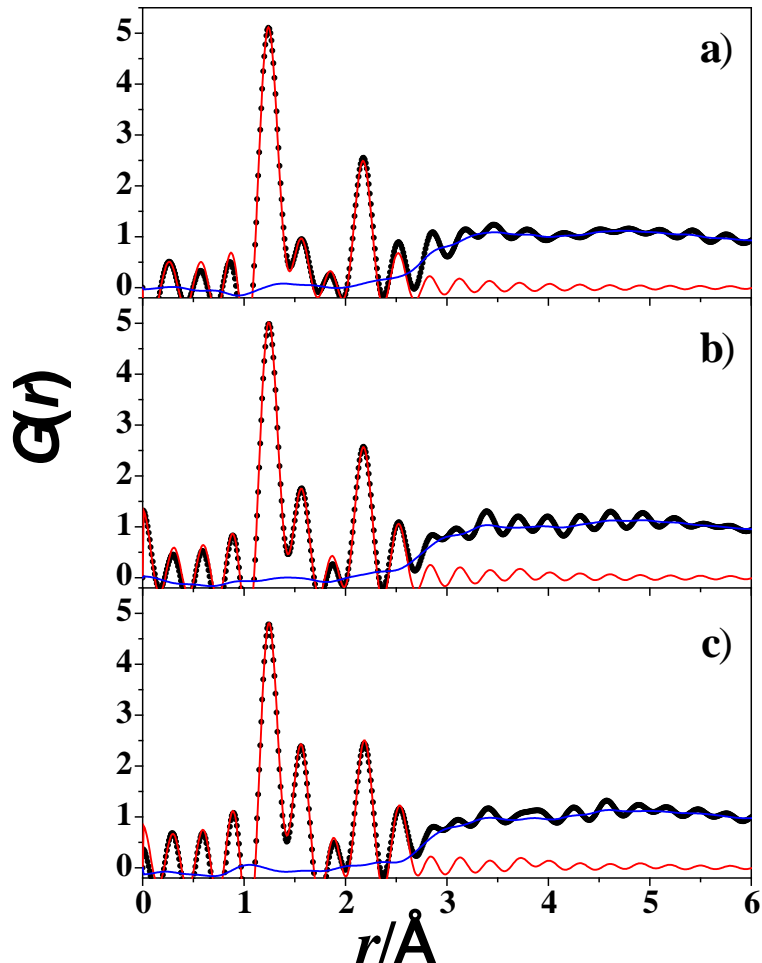


**Figure S7.** Total X-ray pair correlation function obtained by HEXRD experiments (black dots). The intra- and the inter-molecular X-ray pair correlation functions are also shown as red and blue lines, respectively for (a)  $[\text{C}_2\text{Am}^+]\text{[NO}_3^-]$ , (b)  $[\text{C}_3\text{Am}^+]\text{[NO}_3^-]$ , and (c)  $[\text{C}_4\text{Am}^+]\text{[NO}_3^-]$ .

**Figure S8.**

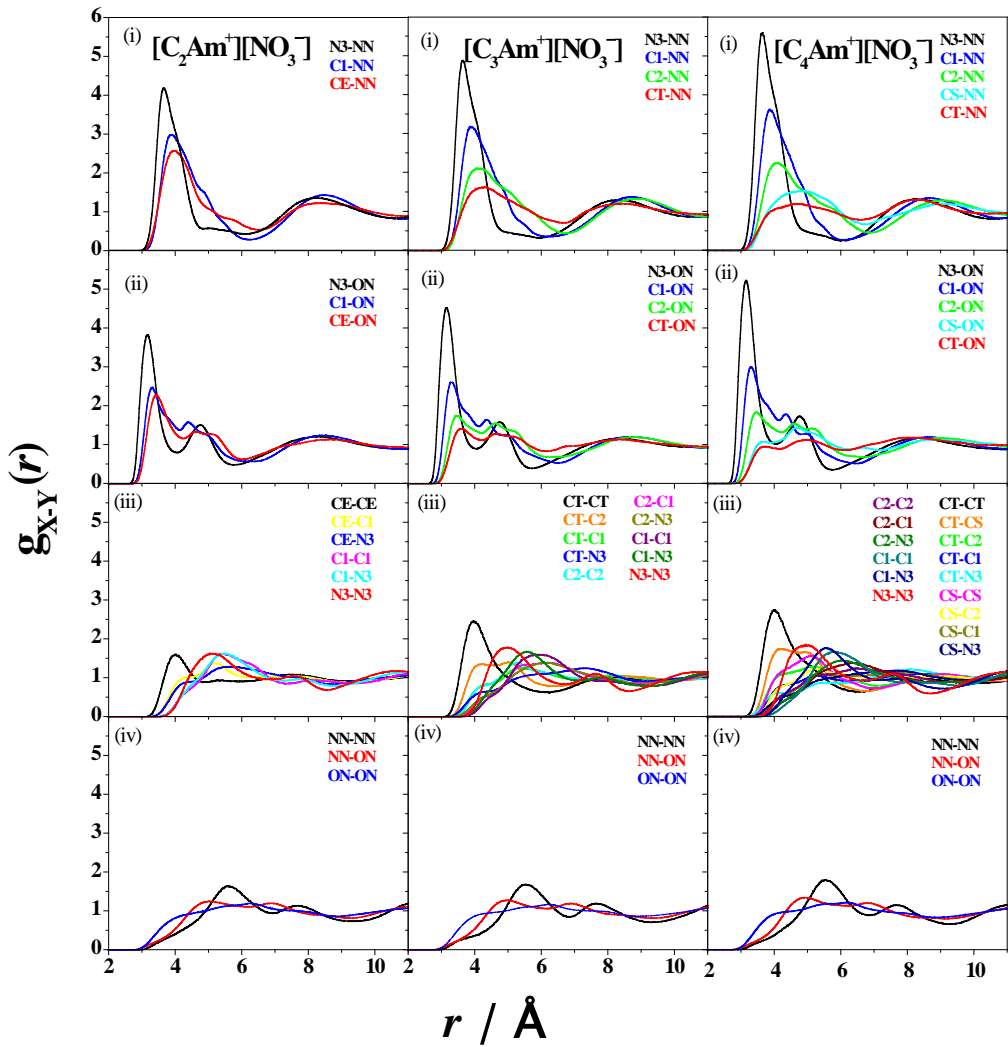


**Figure S8.** Partial atom-atom pair correlation function  $g_{X-Y}(r)$  for the (i) cation-anion(NN), (ii) cation-anion(ON), (iii) cation-cation, (iv) anion-anion, respectively.

**Figure S9.**

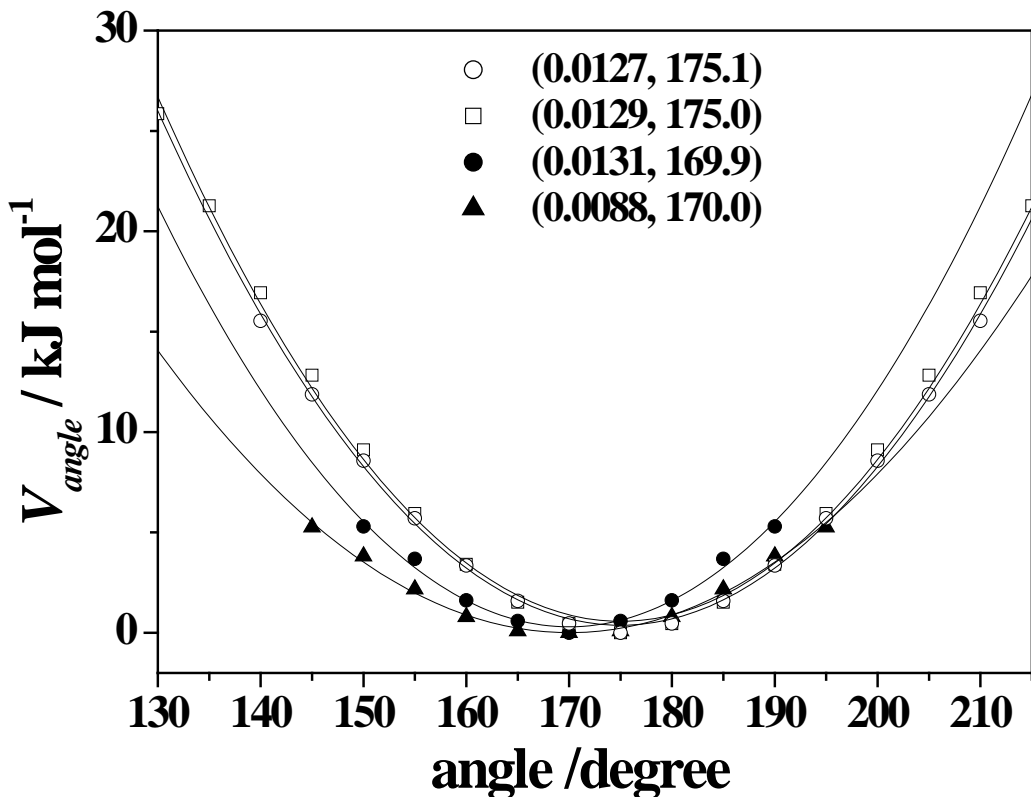


**Figure S9.** Potential energy surface (PES) as a function of the N-H-O bond angle, angle  $\theta$  for  $\text{C}_2\text{H}_5(\text{H}_2)\text{N}\cdots\text{HONO}_2$  molecular complexes in gas phase ( $\circ$ ), in chloroform ( $\square$ ), and  $\text{C}_2\text{Am}^+\cdots\text{NO}_3^-$  ion pairs in chloroform ( $\bullet$ ), in acetonitrile ( $\blacktriangle$ ). Solid lines represent calculated values with the refined parameters of  $k_\theta$  and  $\theta_0$  using  $V_{\text{angle}} = k_\theta(\theta - \theta_0)^2$ , the values for which are shown in parentheses as  $(k\theta, \theta_0)$ .